Journal of Food Engineering 112 (2012) 274–281

Contents lists available at SciVerse ScienceDirect

Journal of Food Engineering

journal homepage: www.elsevier.com/locate/jfoodeng

# A mathematical model describing the two stages of low-pressure-vaporization of free water

C.M. Augusto *, J.B. Ribeiro, A.R. Gaspar, V.R. Ferreira, J.J. Costa

*ADAI–LAETA, Department of Mechanical Engineering, University of Coimbra, Rua Luís Reis Santos, Pólo II, 3030-788 Coimbra, Portugal*

ARTICLE INFO

*Article history:*
Received 7 March 2012
Accepted 9 May 2012
Available online 17 May 2012

*Keywords:*
Low-pressure-vaporization
Flash boiling
Water vaporization modeling

ABSTRACT

This paper reports the development and application of a mathematical model for the prediction of the low-pressure-vaporization (LPV) process of free water. The study is focused on defining clearly the two stages of the LPV process (before and after the so-called flash point) and on evaluating their contribution for the overall transient evolution of the relevant parameters.

The physical domain was divided into two control volumes: the first one contains the mass of free water, ideally assumed at a uniform temperature; the second one includes the volume of the vaporization chamber above the water free surface, the condenser and the vacuum pump. The governing differential equations of the model were solved by the Euler method using the *EES-Engineering Equation Solver*.

The results obtained show that the mathematical model describes the complete process of low-pressure-vaporization of free water, giving evidence to the weight of the first stage on the process transient evolution.



## 1. Introduction

The low-pressure-vaporization (LPV) of water is accompanied by evaporation from the free surface and by bulk vaporization whenever pressure decreases to a value well below the saturation pressure. The great amount of energy required by the water vaporization – the latent heat of phase change – is taken from the mass of water itself. The low-pressure-vaporization occurs in two distinct stages as pressure is gradually decreased: an initial period, with just evaporation at the free surface, while the air is being removed from its surroundings, and a second stage that suddenly begins when pressure drops below the saturation value and the water starts boiling (*flash point*). This second stage may be called *flash boiling* and it is responsible for the majority of the vapor production.

The LPV process has been differently defined and characterized by several authors according to its applications. Saury et al. (2002) studied this process, although calling it *flash evaporation*, and analyzed the flashing time and the vaporized mass of a water film. They evidenced the importance of this phenomenon for several applications and showed that the vaporization flow rate by *flash evaporation* is more significant than during simple vaporization. Likewise, Aoki (2000) made a detailed analysis of water *flash evaporation* under low-pressure, by studying the maximum heat flux and the maximum heat transfer coefficient, and emphasizing their relevance to the global phenomenon.

Several authors (Lai et al., 2004; Huang and Lai, 2010) focus their studies specifically on the development of technologies to enhance the water vaporization. The LPV could be a promising technique for this aim. Muthunayagam et al. (2005) have used the low-pressure-vaporization of saline water for the production of fresh water, and they achieved a yield between 3% and 4%.

Another relevant application the LPV can be in the field of refrigeration, mainly in the area of food processing, presenting numerous advantages over conventional technologies, namely on the process duration and on a smaller energy consumption (McDonald and Sun, 2000; Sun and Zheng, 2006). Moreover, the improvement of the quality and safety of products by this method increases their shelf life, a feature that has encouraged studies towards the use of this technology to various food sectors. For instance, this process has been widely used in the fruit and vegetable industry, such as lettuce and sweet corn, and extensively studied for cooked beef (McDonald and Sun, 2000; Donald et al., 2002; Jin, 2007; Sun and Wang, 2004; Donald and Sun, 2001). Wang and Sun (2004) evaluated the effect of the operating conditions on low-pressure refrigeration of cooked meat, concluding that the process evolution depends on three important parameters: the chamber free volume, the pumping speed and the condenser temperature.

The phenomenon of LPV of water has also been employed in the drying technology. Drying of fruits, vegetables and agriculture materials is operated using the LPV phenomenon integrated with other technologies (Nimmol et al., 2007; Bazyma et al., 2006). For example, Nimmol et al. (2007) described a technology combining

* Corresponding author. Tel.: +351 239 790 700; fax: +351 239 790 701.
*E-mail address:* catia.augusto@dem.uc.pt (C.M. Augusto).

0260-8774/$ - see front matter © 2012 Elsevier Ltd. All rights reserved.
http://dx.doi.org/10.1016/j.jfoodeng.2012.05.013

**Nomenclature**

| | |
|---|---|
| $A$ | surface area ($m^2$) |
| $c_p$ | specific heat (J $kg^{-1}$ $K^{-1}$) |
| CV1, CV2 | control volumes in the physical model |
| $D$ | diffusion coefficient ($m^2$ $s^{-1}$) |
| $h_{fg}$ | latent heat of vaporization of the water (J $kg^{-1}$) |
| $\dot{m}_a$ | rate of change of the mass of air (kg $s^{-1}$) |
| $\dot{m}_v$ | rate of change of the water vapor mass (kg $s^{-1}$) |
| $\dot{m}_{v,cd}$ | mass flow rate of the condensed vapor (kg $s^{-1}$) |
| $\dot{m}_{v,i}$ | mass flow rate of vapor into CV2 (generated in CV1) (kg $s^{-1}$) |
| $\dot{m}_{v,o}$ | mass flow rate of vapor out of CV2 (kg $s^{-1}$) |
| $\dot{m}_{v,vp}$ | mass flow rate of vapor extracted by the vacuum pump (kg $s^{-1}$) |
| $m_w$ | initial mass of water (kg) |
| $M_a$ | molecular weight of the air = 28.97 (kg $kmol^{-1}$) |
| $M_v$ | molecular weight of water vapor = 18.015 (kg $kmol^{-1}$) |
| $P$ | total pressure (Pa) |
| $P_a$ | partial pressure of the air (Pa) |
| $P_{sat}$ | saturation pressure (Pa) |
| $P_{v,t}$ | threshold pressure level (Pa) |
| $P_v$ | partial pressure of the water vapor (Pa) |
| $R$ | universal ideal gas constant = 8314.5 (J $kmol^{-1}$ $K^{-1}$) |
| $t$ | time (s) |
| $T_c$ | chamber temperature (K) or (°C) |
| $T_{cd}$ | condenser temperature (K) or (°C) |
| $T_w$ | liquid water temperature (K) or (°C) |
| $t_{FP}$ | time for the flash point (s) |
| $\dot{V}_e$ | volume flow rate of the pump ($m^3$ $s^{-1}$) |
| $V_f$ | free volume of the vaporization chamber ($m^3$) |
| $V_{vc}$ | volume of the vaporization chamber ($m^3$) |
| $V_{m_w}$ | volume occupied by the liquid water ($m^3$) |

*Subscripts*

| | |
|---|---|
| *0* | initial condition |
| *cd* | condenser |
| *i* | into CV2 |
| *o* | out of CV2 |
| $V_p$ | vacuum pump |
| *w* | liquid water |

*Greek symbols*

| | |
|---|---|
| $\Delta t$ | integration time step (s) |
| $\Delta z$ | thickness of diffusion layer (m) |
| $\rho$ | density (kg $m^{-3}$) |
| $\rho_a$ | air density (kg $m^{-3}$) |
| $\rho_v$ | vapor density (kg $m^{-3}$) |

the LPV phenomenon with superheated steam and far-infrared radiation for drying banana – a product that is rather sensitive to heat. They argue that the traditional technology – hot air drying – is a very energy-intensive operation and leads to great degradation of the product quality due to elevated drying temperature and the presence of oxygen in the drying system. As a result, this study showed a final product with more crispness, especially at higher temperatures.

As in other multiparametric processes, the study and optimization of LPV benefits from numerical simulations. Several researchers developed mathematical models and conducted numerical studies to simulate the phenomena of the LPV (Dostal, 2002; Jin and Xu, 2006b; Aoki, 2000; Muthunayagam et al., 2005).

Jin and Xu (2006a) and Aoki (2000) developed detailed and complete mathematical models to simulate the LPV of water. Nevertheless, these models could not distinguish between the two characteristic stages of the LPV process. The first stage, however, may have a significant importance in the overall transient evolution of the process and so it cannot be ignored. The present work aims to give a step forward in the numerical modeling of the LPV phenomena of free water, proposing a model that differentiates the two characteristic stages of the process. This model describes minutely all transport phenomena as well as the physics of the process.

## 2. Modeling of the low-pressure-vaporization phenomena

### 2.1. Physical model

The LPV system considered for this study is schematically shown in Fig. 1. As typically, it comprises three major components: a vaporization chamber (VC); a vacuum pump (VP) and a vapor condenser (CD). The low-pressure required in the vaporization chamber that contains the water is achieved with the vacuum

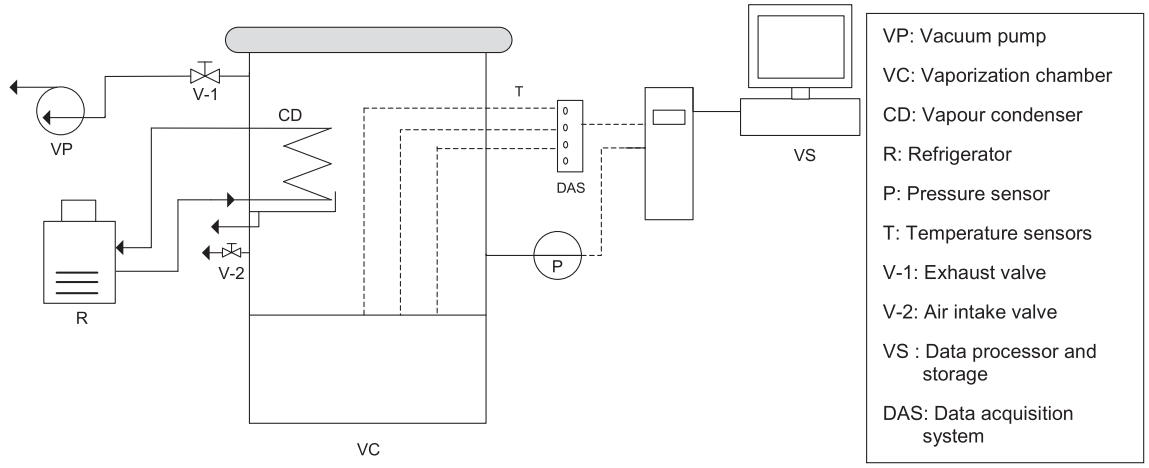


**Fig. 1.** Schematic diagram of a low-pressure-vaporization system (adapted from Saury et al., 2002).

pump. In the initial stage, while the total pressure within the chamber is above the saturation pressure of water, the evaporation at the free surface is ruled by the diffusion of the water vapor in the still air existing in the chamber (Cioulachtjian et al., 2010). Although the energy necessary for the vaporization is taken from the water itself, its temperature will not decrease significantly in this period, because the amount of water vapor produced in this stage is relatively small.

When the total pressure within the vaporization chamber reaches the water saturation pressure, the vapor production starts being governed by the boiling process and the diffusion component becomes irrelevant. This moment is designated the *flash point*. As the pressure of the water vapor drops below the saturation pressure by the action of the vacuum pump, the liquid water vaporizes to compensate that drop. Consequently, the water temperature (and likely the saturation pressure) starts to decrease substantially. At this stage the rate of pressure reduction can be significantly enhanced by capturing part of the generated water vapor in a condenser.

As it is clear from this description, the initial stage of the LPV has a minor importance in the parameters evolution and for this reason is usually skipped in the simulations of the process. However, the initial stage is known to have a non negligible importance in the total process duration (Saury et al., 2002; Cheng and Lin, 2007).

### 2.2. Mathematical model

For modeling proposes, the LPV system was divided into two control volumes (CV) as shown in Fig. 2. The first one comprises the mass of water (1.5 kg, see Table 1). The water is considered ideally mixed with a uniform temperature throughout its volume. The CV2 defines the region of the vaporization chamber above the water free surface. The properties of the air and of the water vapor in this region are taken as homogeneous. Within this CV are included the condenser and the vacuum pump, both acting as mass sinks. As in the preceding one, the properties of the air–vapor mixture throughout this volume are considered uniform. Both control volumes are considered adiabatic and assumed to be in equilibrium with each other. This means assuming that there is thermodynamic equilibrium between gaseous and liquid phases, so that the two phases are instantaneously at the same temperature.

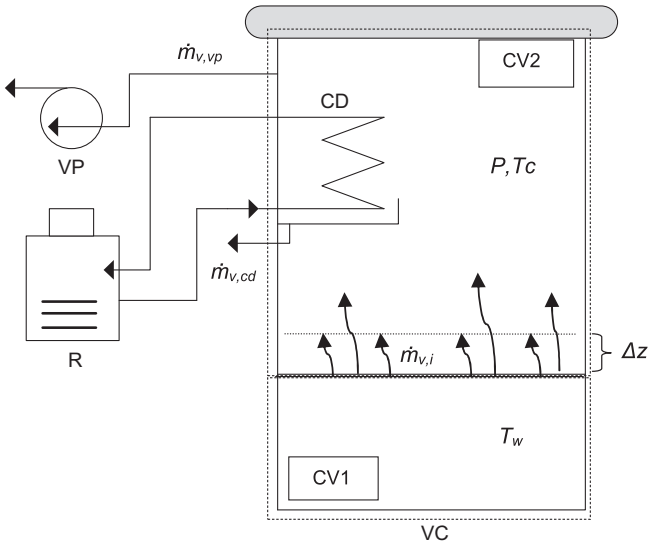


**Fig. 2.** Schematic diagram of the physical model.

**Table 1**
Specific operating conditions of the low-pressure-vaporization process.

| | | |
|---|---|---|
| Volume flow rate of the pump | $\dot{V}_e$($m^3\ s^{-1}$) | 0.0033 |
| Volume of the vaporization chamber | $V_{vc}$ ($m^3$) | 0.017 |
| Initial mass of water | $m_w$ (kg) | 1.5 |
| Initial chamber temperature | $T_{vc,o}$ (°C) | 25 |
| Initial water temperature | $T_{w,0}$ (°C) | 25 |
| Condenser temperature | $T_{cd}$ (°C) | 1 |
| Initial vapor partial pressure | $P_{v,o}$ (Pa) | 0.5 $P_{sat,0}$ |
| Initial total pressure | $P_0$ (Pa) | 101325 |

The temperature of liquid water determines the saturation pressure within CV2. However, the temperature of the water depends on the mass of the water vaporized and it will be determined by applying coupled mass and energy balances to CV1. The vapor pressure within the CV2 is, in turn, used to estimate the vaporization rate, which, during the first stage of the process, depends directly on the vapor pressure gradient across the diffusion layer. So, whenever the vapor pressure in CV2 drops below the saturation pressure, the water from the CV1 vaporizes aiming to raise the vapor pressure towards equilibrium with the saturation value. As referred before, it is this vaporization process that takes out the energy from the liquid phase and produces its temperature decrease.

The total pressure ($P$) in the vaporization chamber (CV2) is the sum of the partial pressures of the air and of the water vapor, respectively $P_a$ and $P_v$:

$$P = P_a + P_v \tag{1}$$

Assuming that the air and the water vapor behave as ideal gases, the rate of variation of the partial pressure of air is defined by:

$$\frac{dP_a}{dt} = \frac{\dot{m}_a R T_c}{M_a V_f} \tag{2}$$

where $R$ is the universal ideal gas constant, $M_a$ is the molar weight of the air and $V_f$ is the free volume of the vaporization chamber $V_f = V_{vc} - V_{m_w}$ (essentially, the space that matches with the CV2).

The rate of change of the mass of air ($\dot{m}_a$) in the chamber corresponds to the mass flow rate of air extracted by the vacuum pump and can be given by the Eq. (3):

$$\dot{m}_a = \frac{dm_a}{dt} = -\dot{V}_e \rho a \tag{3}$$

where $\dot{V}_e$, the volume flow rate of the pump, is considered constant and taken equal to the value shown in Table 1 and $\rho_a$, the density of air, is given by:

$$\rho_a = \frac{P_a M_a}{R.T_c} \tag{4}$$

Thus, replacing Eqs. (3) and (4) in Eq. (2), the rate of variation of the partial pressure of air is given by:

$$\frac{dP_a}{dt} = -\frac{\dot{V}_e P_a}{V_f} \tag{5}$$

Similarly, the variation rate of the vapor partial pressure is calculated by:

$$\frac{dP_v}{dt} = \frac{\dot{m}_v R T_c}{M_v V_f} \tag{6}$$

where $M_{v,}$ is the molar mass of the vapor and $\dot{m}_v$ is the rate of change of the mass of water vapor in the chamber, CV2, given by:

$$\dot{m}_v = \frac{d\dot{m}_v}{dt} = \dot{m}_{v,i} - \dot{m}_{v,o} \tag{7}$$

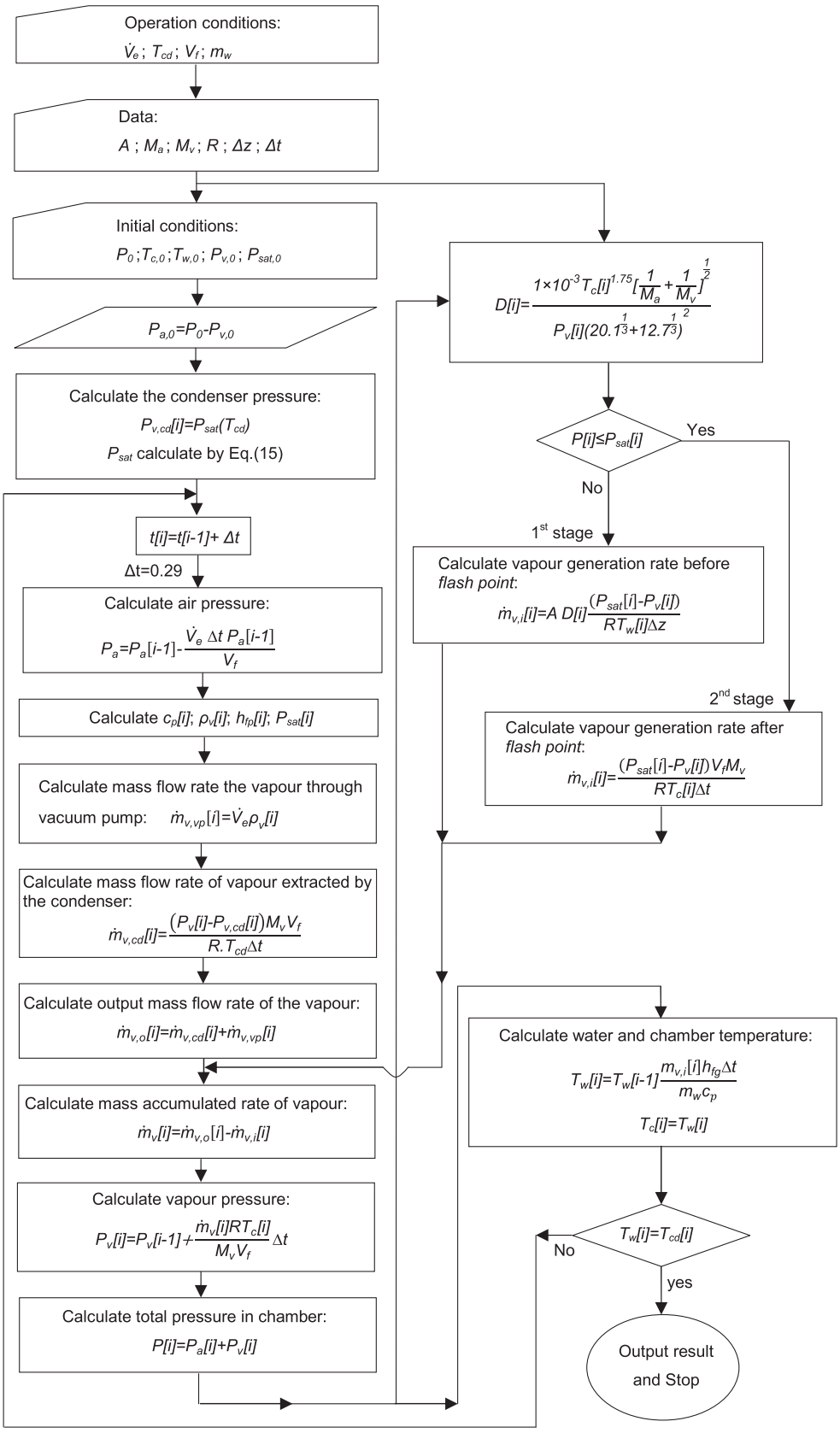


**Fig. 3.** Flow chart of the simulation program.

The mass flow rate of outcoming vapor ($\dot{m}_{v,o}$) is given by:

$$\dot{m}_{v,o}=\dot{m}_{v,c,d}+\dot{m}_{v,vp} \tag{8}$$

where $\dot{m}_{v,cd}$ is the mass flow rate of water vapor removed by the condenser and $\dot{m}_{v,vp}$ is the mass flow rate of vapor extracted by the vacuum pump, calculated by:

$$\dot{m}_{v,vp} = \dot{V}_e \rho_v \tag{9}$$

Given the typical values of the pump volume flow rate and of the vapor density, the mass flow rate of the vapor taken out from the system by the pump is small, and its value determines the vaporization rate. It is normally found that the use of only one typical vacuum pump is not enough to meet the purposes intended for a high vaporization rate. This problem is usually solved with the inclusion of a condenser in the system. In this model, at each integration step, the condenser will reduce the vapor pressure in CV2 towards the saturation pressure at the condenser operating temperature, thus acting as an additional vapor sink. It should be noted, however, that at the beginning of each integration step, due vaporization from CV1, the vapor pressure within CV2 will be higher than the saturation pressure at the condenser temperature. The mass flow rate of the vapor removed from the system by the condenser is given by

$$\dot{m}_{v,cd} = \frac{\partial}{\partial t}\left[\frac{(P_v - P_{v,cd})M_v V_f}{R.T_{cd}}\right] \tag{10}$$

where $P_{v,cd}$ is equal to the saturation pressure of water at the condenser temperature ($T_{cd}$) and the vapor density is given by

$$\rho_v = \frac{\rho_v M_v}{R.T_c} \tag{11}$$

As stated before, the pressure reduction in CV2 is responsible for the vaporization of water in CV1. Before the *flash point*, i.e., while the total pressure in CV1 is still above the saturation pressure of the water, due to a still significant fraction of air existing in the gaseous mixture contained in CV2, the vaporization occurs mainly by diffusion at the water free surface. In that case, the vapor generation rate ($\dot{m}_{v,i}$) is a function of the vapor partial pressure in the vaporization chamber (CV2) and the water temperature. After Fick's law of diffusion, it may be expressed by (Mills, 1995):

$$\dot{m}_{v,i} = -AD\frac{M_v}{RT_w}\frac{\partial P_v}{\partial z} \tag{12}$$

where $A$ is the free-surface area and $\partial P_v/\partial z$ is the vapor pressure gradient at the water surface. The diffusion coefficient of water vapor in the air, $D$, is given by the Fuller–Schettler–Giddings equation (Quick et al., 2009):

$$D = \frac{1\times 10^{-7} T_c^{1.75}\left(\frac{1}{M_a}+\frac{1}{M_v}\right)^{\frac{1}{2}}}{P_v\left(20.1^{\frac{1}{3}}+12.7^{\frac{1}{3}}\right)^2} \tag{13}$$

In the second stage of the process (after the *flash point*), the rate of vapor generation is mostly determined by the difference between the saturation pressure, at the liquid water temperature, and the vapor pressure in CV2, and it may be represented by:

$$\dot{m}_{v,i} = \frac{\partial}{\partial t}\left[\frac{(P_{sat} - P_v)V_f M_v}{RT_c}\right] \tag{14}$$

and the saturation pressure of the water $P_{sat}$ is estimated by the Antoine equation (Poling et al., 2001):

$$P_{sat} = e^{\left(23.209 - \frac{3816.44}{T_w - 46.44}\right)} \tag{15}$$

The time evolution of the water temperature is estimated after an energy balance to the CV1 one, expressed by:

$$m_w c_p \frac{dT_w}{dt} = -\dot{m}_{v,i} h_{fg} \tag{16}$$

where $c_p$ is the specific heat capacity and $h_{fg}$ is latent heat of vaporization of the water. The mass of water ($m_w$) is assumed as being constant because the amount of vaporized water is small comparatively with the initial mass. Other authors, like Wang and Sun (2002), adopted the same simplification. All the thermophysical properties of water considered in the equations shown above are varying with the thermodynamic conditions of the system.

The initial conditions considered for the system are listed in Table 1.

### 2.3. Numerical solution procedure

The model equations were solved using the *EES-Engineering Equation Solver* (Klein, 2004), a computer program to numerically solve algebraic equations that has many built-in mathematical and thermophysical properties functions.

The algorithm to solve the equations used in this model is schematically represented in Fig. 3. In the present configuration, the temperature is used as the stop criterion: when the water temperature ($T_w$) is equal to the condenser temperature ($T_{cd}$), the simulation stops. The differential equations were solved using the Euler method in an iterative procedure as sketched in the flowchart of Fig. 3. The calculation is made in two stages according to the value of the chamber pressure. When the total pressure equals the saturation pressure (*flash point*), the second stage of the process begins. The main difference between the first and second stages is the way how the rate of vapor generation is calculated (vd. Section 2.2). The free-surface area is 0.0015 m$^2$, and the diffusion layer thickness $\Delta z$ was assigned a value of 0.025 m after a preliminary study described next.

### 2.4. Thickness of the diffusion layer

For the numerical solution of Eq. (12), the pressure gradient is approached by finite differences, which is equivalent to a piecewise linear representation: $\Delta P/\Delta z$. The driving potential $\Delta P$ is taken as the difference between $P_{sat}$, which is determined by the liquid water temperature, and the vapor partial pressure $P_v$ in CV2, which in the first stage will rapidly drop to a threshold level, $P_{v,t}$, closely below the saturation pressure at the condenser temperature (e.g., ~659 Pa, for $T_{cd}$ = 1 °C). A sensitivity analysis was performed regarding the influence of the diffusion layer thickness, $\Delta z$, on that threshold pressure level $P_{v,t}$. The results presented in Fig. 4 show an asymptotic decrease of that influence on the model output, which reaches independence at about $\Delta z$ = 0.025 m, a value that was assumed to be adequate for the thickness of the diffusion layer and thus used in all subsequent calculations.

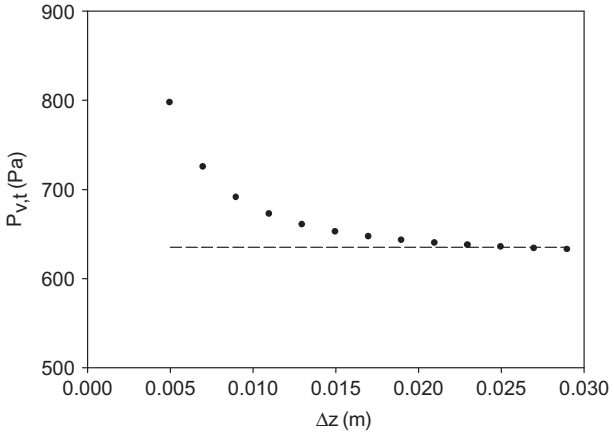


**Fig. 4.** Tests for $\Delta z$ independence of the model, monitoring the influence on the threshold pressure level $P_{v,t}$ predicted in the first stage. The dashed line represents the $P_{v,t}$ level for $\Delta z$ = 0.025 m.

## 3. Results and discussion

The most innovative aspect of the present model consists of the representation of both stages of the LPV process (before and after the *flash point*). The results of the model are analyzed in terms of their physical realism by conducting a parametric study and a comparison with published experimental data.

Fig. 5a presents the predicted time evolution of the water temperature considering the operating conditions listed in Table 1, with a clear definition of each of the two stages. After the flash point, the water temperature drops sharply, resulting in a decrease of approximately 24 degrees in 150 s. Other authors (Dostal, 2002; Dostal and Petera, 2004a) obtained similar results, although using other initial and operating conditions. The great difference in the present results is the presence of the first stage that lasts for about 18 s. It is possible to see that this stage has an expressive contribution to the total process duration, in spite of its almost insignificant effect on the water temperature decrease. This was expected because in this stage the vaporization rate is governed by diffusion transport phenomena.

Fig. 5b shows the time variations of the vapor partial pressure and of the saturation pressure of the free water. As observed for the temperature, the two distinct stages of the vaporization process are evident. When the process starts, the vapor partial pressure $P_v$ decreases sharply due to the combined effect of the vacuum pump and the condenser, stabilizing at a threshold value $P_{v,t}$ slightly below the saturation pressure at the condenser temperature ($P_{v,cd}$ = 659 Pa). At this stage, the vaporization rate is very low, as it is governed by diffusion only. Simultaneously, the total pressure $P$ in the chamber decreases due essentially to the removal of air. When $P$ drops below the saturation pressure of the liquid water, the spontaneous onset of boiling (the *flash point*) is observed, producing step changes of both the vapor partial pressure $P_v$ (see Fig. 5b) and the vaporization rate $\dot{m}_{v,i}$ (from $1.7 \times 10^{-5}$ to $1.2 \times 10^{-3}$ kg s$^{-1}$, v. Fig. 5c). This results in a sudden increase of the total pressure $P$ in the chamber, as it can be seen in Fig. 5d. The order of magnitude of such changes is typical of this kind of process; however the precise values depend on the system characteristics.

A parametric study was then performed to analyze the effects of varying the condenser temperature $T_{cd}$, the mass of water $m_w$ and the vacuum pump flow rate $\dot{V}_e$ on the time variation of both the water temperature $T_w$ and the vapor pressure $P_v$; the results are plotted in Figs. 6–8.

It is seen that although not having a significant influence on the time to the flash point $t_{FP}$, the temperature of the condenser $T_{cd}$ has a relevant effect on the final temperature of the water, as evidenced in Fig. 6. This results from the fact that the vapor partial pressure $P_v$ in the vacuum chamber tends asymptotically to the value of the saturation pressure at the condenser temperature ($P_{v,cd}$). It is seen that the lower the condenser temperature, the higher the vaporization rate and likewise the water temperature decrease. It is possible to conclude that high vaporization rates are not possible to achieve without a condenser (or a similar effect), since the vapor partial pressure in the chamber would then be only ruled by the vacuum pump.

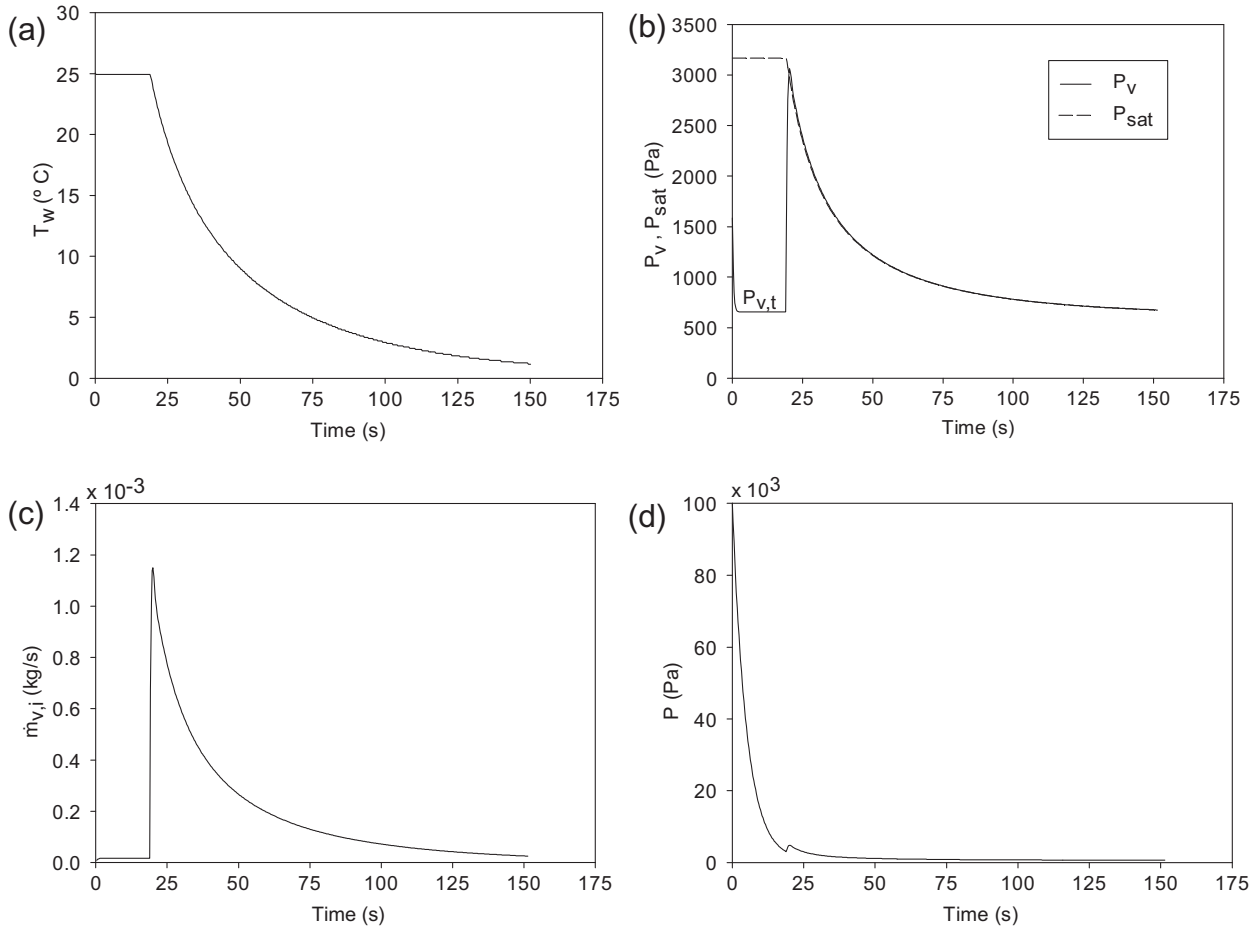


**Fig. 5.** Evolution of the LPV parameters: (a) water temperature; (b) vapor partial and saturation pressures; (c) vapor generation rate; (d) total pressure in the vaporization chamber.

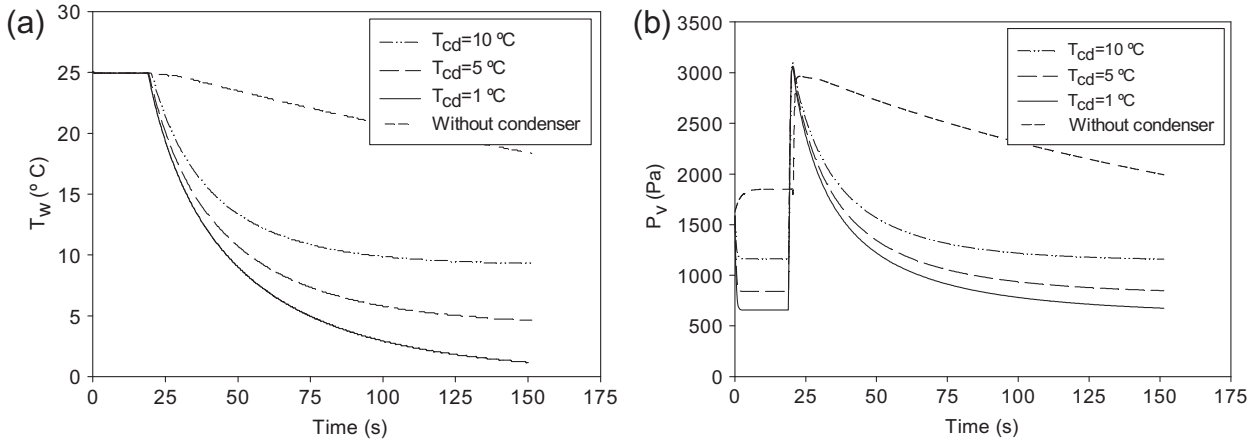


**Fig. 6.** Evolutions of: (a) the water temperature and (b) the vapor partial pressure for three different condenser temperatures.

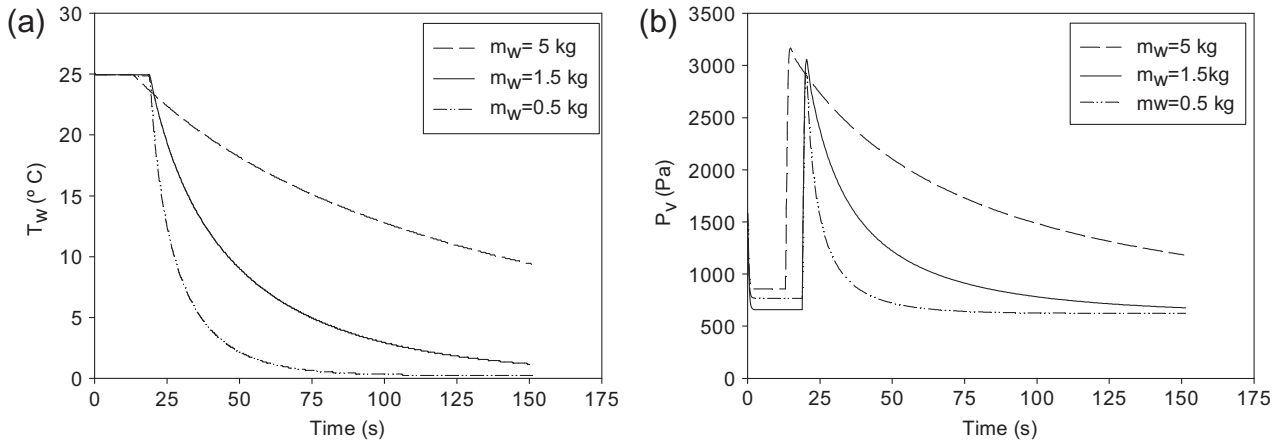


**Fig. 7.** Evolutions of: (a) the water temperature and (b) the vapor partial pressure for three different masses of water.

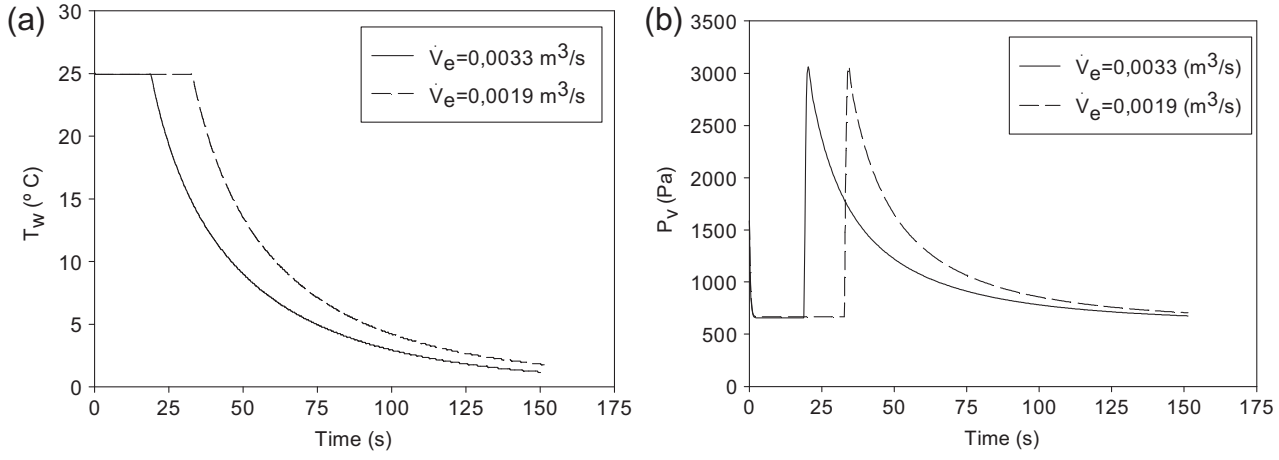


**Fig. 8.** Evolution of: (a) the water temperature and of (b) the vapor partial pressure for two volume flow rates of the pump.

On the other hand, Fig. 7 shows that the final values of the water temperature and of the vapor partial pressure, as well as the time to the flash point depend greatly on the mass of free water. As expected, the lower the heat capacity of the contained water, the lower will be the achieved temperature of the water after a given period (e.g., 150 s). However, as the curves for $m_w$ = 0.5 and 1.5 kg already suggest, $T_w$ would always tend to $T_{cd}$, if $t \to \infty$. The different values obtained for the time to the flash point $t_{FP}$ depend only on the free volume within the vaporization chamber and thus on the initial volume of air that must be removed.

The effects of the volume flow rate of the vacuum pump on the time variations of the water temperature and of the vapor partial pressure can be observed in the graphics of Fig. 8. The pump flow rate has an important effect on the time to the flash point and

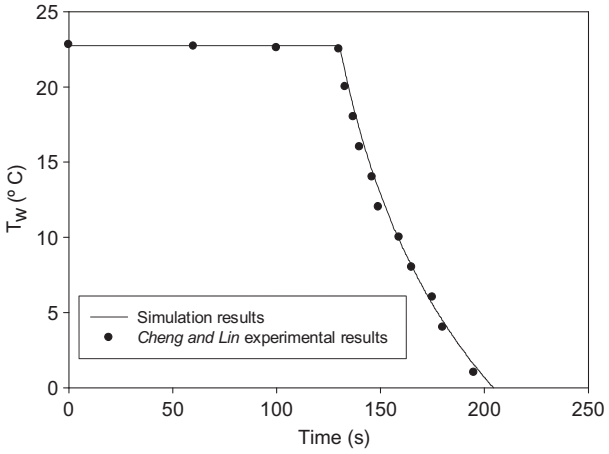


**Fig. 9.** Evolution of the water temperature: comparison between present simulation and the experimental results of Cheng and Lin, 2007.

consequently a relevant influence on the global evolution of all parameters of the LPV process (water temperature, vapor pressure and vaporization rate).

Finally, a validation study was performed taking as a reference the experimental results of Cheng and Lin (2007). Since some characteristic data of the experimental set-up were not provided by these authors – namely the volume flow rate of the pump ($\dot{V}_e$) and the free volume of the vaporization chamber ($V_f$) – and as the value of $\dot{V}_e$ is determinant for the duration of the first stage, the following strategy was adopted to somehow overcome the lack of those data. Using the same mass of water and the same temperature of the condenser mentioned by Cheng and Lin (2007), and considering the same free volume $V_f$ as in the previous calculations, a series of runs was performed changing the pump volume flow rate in order to search for the value of $\dot{V}_e$ that allows predicting the same flash point time (about 130 s) as reported by Cheng and Lin, 2007. With these data, the water temperature evolution predicted by the present model shows a good agreement with the experimental results as it can be seen in Fig. 9.

## 4. Conclusions

In this work a mathematical model for the prediction of the process of low-pressure-vaporization (LPV) of free water was described with its two characteristic stages.

The results show that the mathematical model developed is able to describe the experimental results for LPV processes available in the literature. The present results indicate that the mass of water contained in the vaporization chamber experiences a temperature decrease of 24 degrees in about 150 s and that the first stage of the LPV process has an expressive contribution for the overall transient process. It is possible to conclude that the process is ruled by the time evolution of the water vapor partial pressure in the chamber, which in turn is governed by the vacuum pump flow rate and mainly by the condenser operating temperature.

The parametric analysis performed in this study allowed to conclude that the flow rate of the vacuum pump has a significant influence on the time to the flash point and that the condenser temperature affects mainly the final conditions (temperature and vapor pressure) as well as the total mass of vaporized water. The initial mass of water has influence on the time to the flash point as well as on the final temperature. Thus, it is possible to conclude that the first stage of process should not be neglected when modeling the LPV of water, since it accounts for a non negligible portion of the overall process duration.

## Acknowledgements

The authors acknowledge the support received from the Foundation for Science and Technology of the Portuguese Ministry of Education and Sciences (Fellowship SFRH/BD/64486/2009).

## References

Aoki, I., 2000. Analysis of characteristics of water flash evaporation under low-pressure conditions. Heat Transfer Asian Res. 29 (1), 22–33.
Bazyma, L.A., Guskov, V.P., Basteev, A.V., Lyashenko, A.M., Lyakhno, V., Kutovoy, V.A., 2006. The investigation of low temperature vacuum drying processes of agricultural materials. J. Food Eng. 74, 410–415.
Cheng, H.-P., Lin, C.-T., 2007. The morphological visualization of the water in vacuum cooling and freezing process. J. Food Eng. 78 (2), 569–576.
Cioulachtjian, S., Launay, S., Boddaert, S., Lallemand, M., 2010. Experimental investigation of water drop evaporation under moist air or saturated vapor conditions. Int. J. Therm. Sci. (Elsevier Masson SAS) 49 (6), 859–866.
Donald, K.M., Sun, D.-W., 2001. Effect of evacuation rate on the vacuum cooling process of a cooked beef product. J. Food Eng. 48 (3), 195–202.
Donald, K.M., Sun, D.-W., Lyng, J.G., 2002. Effect of vacuum cooling on the thermophysical properties of a cooked beef product. J. Food Eng. 52 (2), 167–176.
Dostal, M., Petera, K., 2004. Vacuum cooling of liquids: mathematical model. J. Food Eng. 61 (4), 533–539.
Dostal, M. & Petera, K. (2002). Vacuum cooling of liquids. In: 15th International Congress of Chemical and Process Engineering CHISA. [CD-ROM]. Prague: Czech Society of Chemical Engineering, 2002, pp. 1–11. ISBN 80-86059-33-2.CHISA Conference, Prague.
Huang, M., Lai, F.C., 2010. Numerical study of EHD-enhanced water evaporation. J. Electrostat. 68, 364–370.
Jin, T.X., 2007. Experimental investigation of the temperature variation in the vacuum chamber during vacuum cooling. J. Food Eng. 78 (1), 333–339.
Jin, T.X., Xu, L., 2006a. Numerical study on the performance of vacuum cooler and evaporation-boiling phenomena during vacuum cooling of cooked meat. Energy Convers. Manag. 47 (13–14), 1830–1842.
Jin, T.X., Xu, L., 2006b. Development and validation of moisture movement model for vacuum cooling of cooked meat. J. Food Eng. 75 (3), 333–339.
Klein, S.A., 2004. Engineering Equation Solver (EES). F-Chart Software, Madison.
Lai, F.C., Huang, M., Wong, D.S., 2004. EHD-enhanced water evaporation. Drying Technol. 22 (3), 597–608.
McDonald, K., Sun, D.-W., 2000. Vacuum cooling technology for the food processing industry: a review. J. Food Eng. 45 (2), 55–65.
Mills, A. F. (1995). In: Irwin (Ed.) Heat and Mass Transfer (pp. 1240). Los Angeles.
Muthunayagam, A.E., Ramamurthi, K., Paden, J.R., 2005. Modelling and experiments on vaporization of saline water at low temperatures and reduced pressures. Appl. Thermal Eng. 25, 941–952.
Nimmol, C., Devahastin, S., Swasdisevi, T., Soponronnarit, S., 2007. Drying of banana slices using combined low-pressure superheated steam and far-infrared radiation. J. Food Eng. 81, 624–633.
Poling, B.E., Prausnitz, J.M., O'Connell, J.P. (Eds.), 2001. The properties of gases and liquids, 5th ed. McGraw-Hill, New York.
Quick, C., Ritzinger, D., Lehnert, W., Hartnig, C., 2009. Characterization of water transport in gas diffusion media. J. Power Sources 190 (1), 110–120.
Saury, D., Harmand, S., Siroux, M., 2002. Experimental study of flash evaporation of a water film. Int. J. Heat Mass Transfer 45, 3447–3457.
Sun, D.-W., Wang, L., 2004. Experimental investigation of performance of vacuum cooling for commercial large cooked meat joints. J. Food Eng. 61 (4), 527–532.
Sun, D.-W., Zheng, L., 2006. Vacuum cooling technology for the agri-food industry: past, present and future. J. Food Eng. 77 (2), 203–214.
Wang, L., Sun, D.-W., 2002. Modelling vacuum cooling process of cooked meat-part 1: analysis of vacuum cooling system. Int. J. Refrig. 25, 854–861.
Wang, L., Sun, D.-W., 2004. Effect of operating conditions of a vacuum cooler on cooling performance for large cooked meat joints. J. Food Eng. 61 (2), 231–240.